



Enhanced filtration performance of Al₂O₃-SiC porous ceramic composite tube depending on microstructure and surface properties

Kai Jiao^{a,b}, Xiangtao Yu^a, Zhangfu Yuan^{a,*}, Yangang Zhang^{a,c}, Jianhua Liu^b

^aCollaborative Innovation Center of Steel Technology, University of Science and Technology Beijing, Beijing 100083, China, Tel. +86-010-62332598; emails: zfyuan2016@ustb.edu.cn (Z. Yuan), zaidengzainian@163.com (K. Jiao), xtyuipe@163.com (X. Yu), zhang.yangang@scinorwater.com (Y. Zhang)

^bEngineering Research Institute, University of Science and Technology Beijing, Beijing 100083, China, Tel. +86-010-62332598; email: liujianhua@metall.ustb.edu.cn

^cBeijing Scinor Water Technology Co., Ltd., Beijing 100083, China

Received 14 August 2018; Accepted 28 December 2018

ABSTRACT

Microstructure and surface charge properties have great effects on the filtration performance of porous ceramic tubes. The SiC-doped Al₂O₃ porous ceramic composite tube was prepared by extrusion. The surface morphology, element compositions and pore distributions were analyzed. The filtration performance was evaluated based on the permeability and surface charge properties. The permeability and tortuosity were calculated with the method of symbolic-graphic combination according to the experimental results. The method is beneficial to the microstructure design of porous ceramic tube for a better separation performance. The results indicate that the Al₂O₃-SiC porous ceramic composite tube has a narrow pore size distribution and uniform porosity. The most probable pore size is 38–39 μm, and the porosity is about 42%. The permeability and tortuosity are 5.79 μm² and 1.90, respectively. The SiC doping into the Al₂O₃ porous ceramic tube results in a stronger negative surface charge and reduces the pH value of isoelectric point. The permeation velocity of oil–water emulsion droplet at pH 7 is higher than that at pH 3, indicating that SiC doping enhances the antifouling performance of Al₂O₃ porous ceramic composite tube.

Keywords: Al₂O₃-SiC porous ceramic composite tube; Porosity; Permeability; Tortuosity; Zeta potential; Antifouling performance

1. Introduction

Water plays a vital role in daily life and industrial production [1]. In recent years, with the increase of population and development of industry, global water resources are becoming shorter and shorter [2–4]. Therefore, various practical solutions have been adopted to conserve water resources [5–7]. In the filtration process of sewages, porous ceramic tubes have gradually become a research hotspot because of their advantages, such as high temperature resistance, corrosion resistance, washing resistance, high mechanical stability, stable structure and narrow pore size distribution, etc. They are very high quality filter materials that can be used

in a variety of harsh conditions and present a good performance on liquid–solid separation [8]. Porous ceramic tubes were restricted because of their expensive production prices. Scholars have looked innovatively for raw materials such as clay, fly ash and apatite that are in abundance to develop low-cost porous ceramic tubes [9–13], which endows porous ceramic tubes with better commercial value.

The separation of porous ceramic tubes is based on the sieve effect to separate the particles of different sizes. Therefore, the separation performance of porous ceramic tubes is closely related to their microstructure, such as pore distribution, porosity and tortuosity [14]. The permeation performance of porous material is usually expressed by

* Corresponding author.

the permeability k that only depends on the microstructure of porous medium and is independent of the liquid nature. The mathematical relationship between the permeability and microstructure of porous material has been reported in literatures [15–17]. However, studies on porous ceramic tubes, which were also porous material, were seldom mentioned. The permeability has a great influence on the filtration and regeneration performance. Therefore, the permeability calculation of porous ceramic tubes based on microstructure parameters is important to their application.

The porous ceramic tubes made of inorganic oxides is electrically charged in aqueous solution due to their amphoteric behavior of surface hydroxyl groups [18,19], and their surface charge properties are usually evaluated by measuring the streaming potential with zeta potential analyzer [20–21]. The filtration performance of porous ceramic tubes depends not only on the simple sieve effect of microstructure but also on the surface charge properties. In the process of removing turbidity particles from oily water, the surface charge properties of porous ceramic tubes and oil droplets seriously affect the antifouling performance of porous ceramic tubes, because the electric charge leads to electrostatic attraction between them, and the attraction causes the pores to be blocked or fouled by oil. It can be found that the sign of zeta potential is more important than its absolute value. The surface charge properties of porous ceramic tube are determined by material. Porous ceramic composite tubes prepared by doping with different materials can effectively enrich their surface functionality and improve their filtration performance.

In this work, a SiC-doped Al_2O_3 porous ceramic composite tube has been fabricated by adding 10 wt% SiC to change the surface properties for a better filtration performance. The surface morphology, element compositions, pore distributions and zeta potential of Al_2O_3 -SiC porous ceramic composite tube were investigated. The relationship between permeability and microstructure parameters was built to help design the microstructure for a better separation performance. Furthermore, the permeability and tortuosity of Al_2O_3 -SiC porous ceramic composite tube were calculated. The permeation experiments of oil–water emulsion droplets at different pH values on the inner surface of Al_2O_3 -SiC porous ceramic composite tube were performed to analyze the effect of SiC doping on the antifouling performance of Al_2O_3 porous ceramic tube.

2. Experimental setup

2.1. Preparation

The SiC-doped Al_2O_3 porous ceramic composite tube was produced by extrusion. α - Al_2O_3 powder (purity >99.5%, Beijing, China), 8 wt% SiC powder (purity >99.5%, Beijing, China), binder (8 wt% starch powder), pore-forming agent (2 wt% charcoal powder), a certain amount of deionized water and TiO_2 were uniformly mixed under strong stir and wet ball-milled into aggregates. The particle sizes of α - Al_2O_3 powder and SiC powder were about 25 μm . pH value of suspension was adjusted to 1.5 by adding 1 mol·L⁻¹ HNO_3 . The aggregates were made into porous ceramic tube by extrusion. After the porous ceramic tube was dried overnight, it was calcined in air under 1,200°C for 12 h.

2.2. Characterization

The morphology of Al_2O_3 -SiC porous ceramic composite tube was observed by scanning electron microscopy (SEM, Quanta FEG 450, USA). The element compositions and distributions of Al_2O_3 -SiC porous ceramic composite tube were characterized by energy dispersive spectroscopy (EDS, TEAM, USA). The surface and bulk pore distributions of Al_2O_3 -SiC porous ceramic composite tube were studied by metalloscope (Olympus BX51M, Japan) and mercury porosimeter (Autopore IV-9500, USA), respectively. The contact angle of droplets was measured by optical contact angle measurement (OCA 15Pro, Germany). The surface charge properties of Al_2O_3 -SiC porous ceramic composite tube and oil–water emulsion droplets were determined by measuring the streaming potential with zeta potential analyzer (ZetaSizer Nano ZS90, England).

2.3. Permeation experiment

In order to study the filtration performance of Al_2O_3 -SiC porous ceramic composite tube, three permeation experiments for each condition were carried out on the inner surface and the average experimental data were used for analysis. Deionized water droplets were used as experimental material to measure the permeability and tortuosity. The oil–water emulsion droplets at pH 3 and 7 were used to study the effect of SiC doping on the antifouling performance of Al_2O_3 porous ceramic tube. The oil–water emulsion was stable, which was obtained by mixing 8 wt% oil, 16 wt% emulsifier (Pure Plant Salufactor, Germany) and 76 wt% deionized water under strong stir. The pH values were adjusted by adding a certain amount of oxalic acid, and they were measured by a pH meter.

A segment of the Al_2O_3 -SiC porous ceramic composite tube was selected randomly. The inner diameter, outer diameter and wall thickness were measured to be 21.61, 31.29 and 9.68 mm, respectively. A high-speed camera (25 frames per second) was used to record the permeation processes of deionized water and oil–water emulsion droplets on the inner surface of Al_2O_3 -SiC porous ceramic composite tubes. The volume of droplets was calculated by Eq. (1) [22] when the contact angle was less than 90°.

$$V_{\text{droplet}} = \pi \left(\frac{L_1^2 L_2}{2} + \frac{L_2^3}{6} \right) + 4rR \left(\frac{\alpha}{2} - \frac{\sin 2\alpha}{4} \right) \quad (1)$$

Fig. 1 is the diagram of droplet permeating on the inner surface of porous ceramic tube when the contact angle is less than 90° and the physical map of Al_2O_3 -SiC porous ceramic composite tube. For the ease of measuring and calculating, Eq. (1) was changed into Eq. (2):

$$V_{\text{droplet}} = \pi \left(\frac{(2L_1)^2 L_2}{8} + \frac{L_2^3}{6} \right) + 2(2L_1) \times R^2 \left(\frac{\arcsin\left(\frac{2L_1}{2R}\right)}{2} - \frac{\sin\left(2\arcsin\left(\frac{2L_1}{2R}\right)\right)}{4} \right) \quad (2)$$

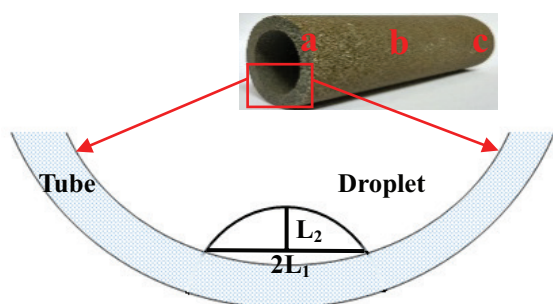


Fig. 1. Diagram of droplet permeating on the inner surface of porous ceramic tube when the contact angle is less than 90° and the physical map of Al_2O_3 -SiC porous ceramic composite tube.

3. Results and discussion

3.1. Microstructure of Al_2O_3 -SiC porous ceramic composite tube

Fig. 2 shows the SEM images of Al_2O_3 -SiC porous ceramic composite tube. The Al_2O_3 -SiC porous ceramic composite tube is formed by stacking and bonding a large number of approximately elongated strips, and the particle sizes are about 100–200 μm . There are a large number of irregular via holes on the surface of Al_2O_3 -SiC porous ceramic composite tube. The three-dimensional pores are transverse connection and longitudinal tortuous extension, which makes the surface morphology very rugged and complicated. It is inferred the Al_2O_3 -SiC porous ceramic composite tube has a good electrostatic adsorption and adherent interception effect on impurities. The pore sizes of Al_2O_3 -SiC porous ceramic composite tube are in the range of 10–80 μm . It is clear that the Al_2O_3 -SiC porous ceramic composite tube is suitable for micron-size particles filtration.

To analyze the element compositions of Al_2O_3 -SiC porous ceramic composite tube, EDS analysis was performed and is shown in Fig. 3. The results indicate that the existence of carbon, oxygen, aluminum and silicon elements in the tube with a weight ratio of 17.69:41.12:40.33:0.62 (C:O:Al:Si). The distributions of aluminum and oxygen, carbon and silicon are similar. The Al_2O_3 -SiC porous ceramic composite tube is mainly composed of Al_2O_3 . It also contains 10 wt% SiC. In addition, a small amount of titanium element comes from the residual sintering additives TiO_2 .

3.2. Pore distributions of Al_2O_3 -SiC porous ceramic composite tube

Pore distribution is the most important property of porous ceramic tubes, which has an immediate impact on permeability, permeation velocity and filtration performance. As shown in Fig. 1, in order to obtain the accurate pore parameters, three segments (left (a), middle (b) and right (c)) of the Al_2O_3 -SiC porous ceramic composite tube were selected to study the pore distributions using metalloscope and mercury porosimeter.

Fig. 4 shows the optical microstructure (OM) binary images of three segments. The black area is pore, and the white area is Al_2O_3 -SiC. Observing the OM images magnified 100 times and comparing the ratio of black area, it is found that the porosity of the left, middle and right segments

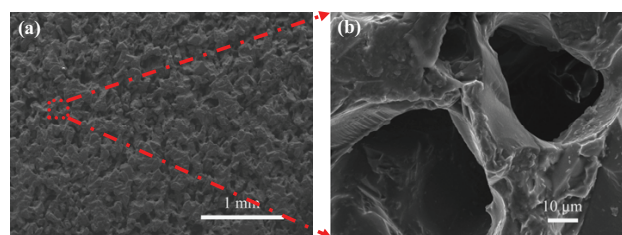


Fig. 2. Micromorphology of Al_2O_3 -SiC porous ceramic composite tube.

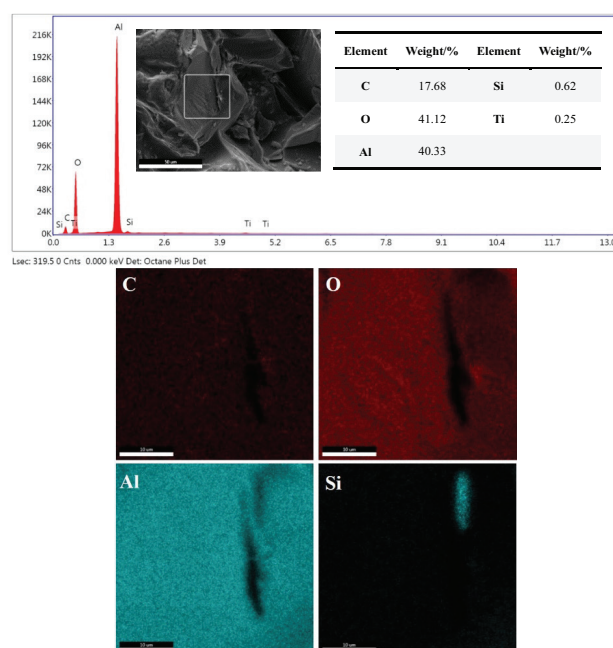


Fig. 3. EDS analysis of Al_2O_3 -SiC porous ceramic composite tube.

are 31.95%, 33.28% and 35.10%, and the average porosity is about 33.44%. The porosity of three segments are very close. The pore distributions are uniform. The average pore size of Al_2O_3 -SiC porous ceramic composite tube observed by metalloscope is about 10–80 μm , which is the same as that observed by SEM.

Fig. 5 shows the bulk pore parameters of three segments measured by mercury porosimeter. The three segments have narrow pore size distributions, and most of their pore sizes are in the range of 20–50 μm . Their most probable pore size are very close, which are about 38–39 μm . The porosity of left, middle and right segment is 42.11%, 41.11% and 40.24%, respectively. It is inferred that the Al_2O_3 -SiC porous ceramic composite tube has a good separation performance.

3.3. Permeability and tortuosity of Al_2O_3 -SiC porous ceramic composite tube

3.3.1. Permeability solution

Table 1 shows the pore structures of Al_2O_3 -SiC porous ceramic composite tube. Fig. 6 shows the volume variation of deionized water droplet during the permeation process according to Eq. (2). The deionized water volume as a

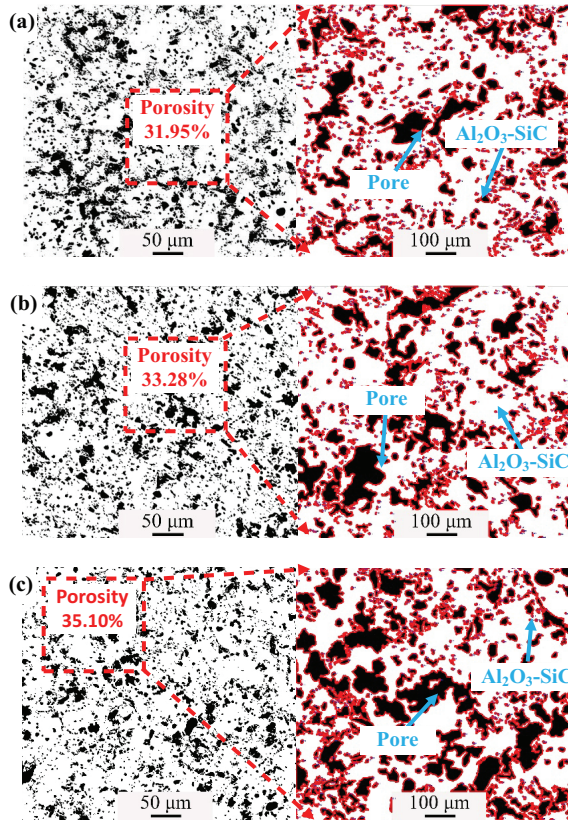


Fig. 4. Optical microstructure (OM) binary images of three segments (left (a), middle (b) and right (c)) of $\text{Al}_2\text{O}_3\text{-SiC}$ porous ceramic composite tube.

function of time is expressed as $V_{\text{droplet}} = -7.9525t + 14.142$, and the permeation velocity is about $7.95 \text{ mm}^3\cdot\text{s}^{-1}$. Fig. 6 shows that with increasing time, the droplet volume linearly reduces, while the permeation velocity is relatively stable. Observing the permeation process of deionized water droplets, it is found that the droplets spread at first and then maintain their spreading range for a period of time until permeating completely.

The permeation velocity of deionized water droplet still maintains at $7.95 \text{ mm}^3\cdot\text{s}^{-1}$ during the permeation process, and the velocity is small enough to meet the condition of Darcy law. According to Darcy's law:

$$Q = \frac{kA\Delta p}{\mu L} \quad (3)$$

where Q is the flow rate. k is the permeability of porous medium. A is the cross-sectional area. Δp is the pressure gradient in the porous media. L is the thickness of porous medium. μ is the viscosity of fluid (The fluid viscosity of deionized water is $\mu = 10^{-3} \text{ Pa}\cdot\text{s}$).

Changing Eq. (3) to Eq. (4):

$$k = \frac{Q\mu}{A\left(\frac{\Delta p}{L}\right)} \quad (4)$$

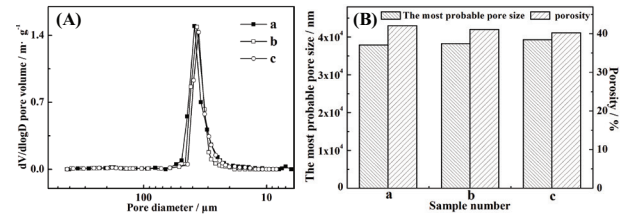


Fig. 5. Bulk pore distributions (A) and pore parameters (B) of three segments (left (a), middle (b) and right (c)) of $\text{Al}_2\text{O}_3\text{-SiC}$ porous ceramic composite tube.

Table 1

Pore structures of $\text{Al}_2\text{O}_3\text{-SiC}$ porous ceramic composite tube

Composition	$\text{Al}_2\text{O}_3\text{-SiC}$
Inner radii, mm	21.61
Outer radii, mm	31.29
Most probable pore size, μm	38–39
Porosity, %	42

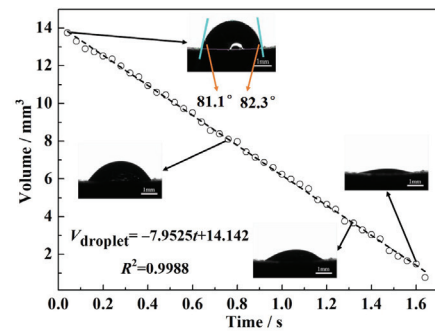


Fig. 6. Volume variation of deionized water during the permeation process.

In this experiment, the permeation process of deionized water under the action of gravity is studied without external pressure. The pressure gradient in the porous ceramic tube is generated by the gravity and capillary force of droplet. The pressure gradient generated by the gravity is $\frac{\Delta p}{L} = \rho g = 0.001 \text{ atm} \cdot \text{cm}^{-1}$. The cross-sectional area of permeation surface (A) and the average value of contact angle (θ) at the initial stage of deionized water permeation process are 0.117 cm^2 and 81.7° , respectively. The pore size is $40 \mu\text{m}$, and the surface tension of water–air is $0.072 \text{ N}\cdot\text{m}^{-1}$ at 23°C . The capillary force is calculated to be $P_c = \frac{2\sigma\cos\theta}{r} = 1039.36 \text{ Pa}$, where σ is the surface tension of two-phase fluid, and θ is the contact angle.

The pressure generated by the gravity is 96.8 Pa . The capillary force is about 10.74 times the gravity. Therefore, the permeability of $\text{Al}_2\text{O}_3\text{-SiC}$ porous ceramic composite tube is $5.79 \mu\text{m}^2$ according to Eq. (4).

3.3.2. Tortuosity solution

It is assumed that the $\text{Al}_2\text{O}_3\text{-SiC}$ porous ceramic composite tube is an ideal porous medium. According to the

generalized Hagen–Poiseuille equation [23], the unit volume flow rate is expressed as:

$$q(r) = nA \frac{\pi \Delta P r^4}{8 L_t \mu} \quad (5)$$

where n is the quantity of tube in a unit area. r is the average hydrological radius of a single tube. q is the flow rate through a single tube. L_t is the true length of tube.

Porosity ϕ is the ratio of pore volume to total volume of porous medium:

$$\phi = \frac{nA\pi r^2 L_t}{AL} \quad (6)$$

Through Eq. (4) to Eq. (6):

$$k = \frac{\phi r^2}{8\tau^2} \quad (7)$$

The tortuosity of Al_2O_3 -SiC porous ceramic composite tube is expressed as:

$$\tau = \sqrt{\frac{\phi r^2}{8k}} = 1.90 \quad (8)$$

The tortuosity is obtained through the experimental data of permeability, porosity and most probable pore size. The calculation results are similar to those in the study by Yu and Li [23]. According to Eq. (7), the permeability of porous ceramic tubes could be predicted by porosity, most probable pore size and tortuosity, providing calculation support for the application of porous ceramic tubes. It is beneficial to the microstructure design for a better separation performance.

3.4. Antifouling performance of Al_2O_3 -SiC porous ceramic composite tube

When the turbidity treatment is carried out on the oily sewages, the oil droplets in the sewages are easily attached to the surface of porous ceramic tube and reduces the tube performance and life. Therefore, in order to study the effect of SiC doping on the antifouling performance of Al_2O_3 porous ceramic tube, the surface charge properties of Al_2O_3 -SiC porous ceramic composite tube and Al_2O_3 porous ceramic tube were measured by streaming potential method, and their pH dependence of zeta potential are shown in Fig. 7. It is found that the isoelectric point (IEP) of Al_2O_3 -SiC porous ceramic composite tube and Al_2O_3 porous ceramic tube are 3.4 and 8.2, respectively. And their zeta potential decreases with the increase of pH value, because the absolute value and sign of zeta potential depend on potential-determining ions in the solution [24]. Fig. 7 shows the doping of SiC into Al_2O_3 porous ceramic tube results in a stronger negative surface charge and a shift of IEP towards lower pH value.

Fig. 8 shows the pH dependence of zeta potential for oil–water emulsion. The zeta potential remains almost steady

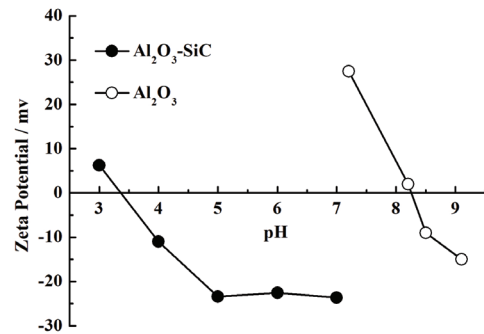


Fig. 7. pH dependence of zeta potential for Al_2O_3 -SiC porous ceramic composite tube and Al_2O_3 porous ceramic composite tube.

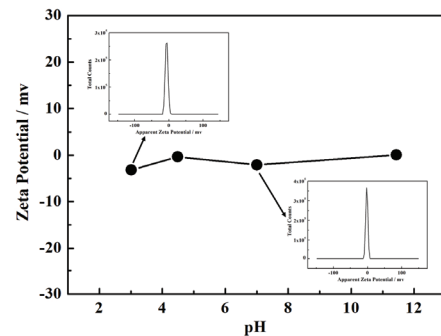


Fig. 8. pH dependence of zeta potential for oil–water emulsion.

from pH 2 to 12. And the zeta potential of oil–water emulsion is approximately -3 mV. The IEP of Al_2O_3 -SiC porous ceramic composite tube is 3.4. When pH value is lower than 3.4, the Al_2O_3 -SiC porous ceramic composite tube has a high positive charge, which is opposite to the charge properties of oil–water emulsion droplets. Electrostatic affinity makes oil–water emulsion droplets easily adsorbed on the surface and pores inner wall of Al_2O_3 -SiC porous ceramic composite tube, causing its pores to be blocked or fouled. When pH value is higher than 3.4, the charge properties of Al_2O_3 -SiC porous ceramic composite tube is the same as those of oil–water emulsion droplets. The repulsive force reduces the adsorption of oil–water emulsion droplets on the surface and pores inner wall of Al_2O_3 -SiC porous ceramic composite tube, producing less fouling.

Fig. 9 shows the volume variation of oil–water emulsion droplets which are obtained by Eq. (2) during the permeation process at pH 3 and 7. The oil–water emulsion droplet has a permeation velocity of $7.15 \text{ mm}^3 \cdot \text{s}^{-1}$ at pH 7, which is faster than that of $4.8455 \text{ mm}^3 \cdot \text{s}^{-1}$ at pH 3. It is indicated that the electrostatic repulsion between the oil–water emulsion at pH 7 and Al_2O_3 -SiC porous ceramic composite tube limits fouling. When the oily sewages are treated to reduce turbidity, they are usually neutral, weakly acidic or weakly alkaline. The surface charge properties of untreated Al_2O_3 porous ceramic tube are a high positive charge, which tends to cause oil droplets to adsorb on the surface of tube and inner wall of pores, furthermore reducing the performance and life. The SiC-doped Al_2O_3 porous ceramic composite tube effectively

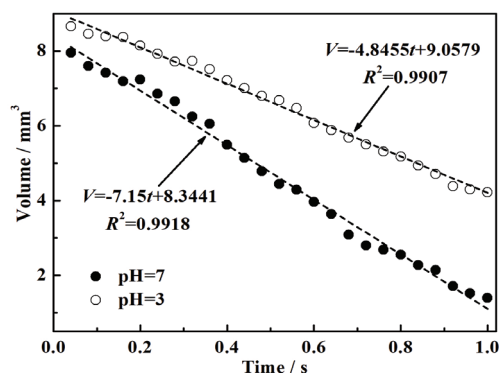


Fig. 9. Volume variation of oil–water emulsion droplets during the permeation process at pH 3 and 7.

improves this phenomenon. The oil–water emulsion droplet has a permeation velocity of 7.15 mm³/s at pH 7, which is less than that of 7.95 mm³/s of deionized water droplet. This is because the viscosity of oil–water emulsion is greater than that of deionized water, resulting in a decrease in the permeation velocity.

4. Conclusions

The SiC-doped Al₂O₃ porous ceramic composite tube with good pore parameters and antifouling performance was successfully prepared by extrusion. The permeability and tortuosity of Al₂O₃-SiC porous ceramic composite tube were calculated through the method provided in this paper, and the method could help design the microstructure of porous ceramic tubes for better separation performance.

The surface charge properties of Al₂O₃ porous ceramic tube and Al₂O₃-SiC porous ceramic composite tube were characterized by measuring the streaming potential. The doping of SiC into Al₂O₃ porous ceramic tube results in a stronger negative charge on the surface of porous ceramic tube, and causes the IEP to shift from 8.3 to 3.4. The oil–water emulsion droplets permeation velocity at pH 7 is faster than that at pH 3, because it is affected by the interaction of the surface of porous ceramic tube and oil–water emulsion. When porous ceramic tubes have the same charge properties as droplets, they will have a higher permeation velocity and a better antifouling performance. The doping of SiC into Al₂O₃ porous ceramic tube effectively enhances its antifouling performance.

Acknowledgment

This research work was partially supported by the National Natural Science Foundation of China (Grant Nos. U1560101 and U1738101) and the National Key Research and Development Program of China (2016YFC0209302).

References

[1] I. Ali, V.K. Gupta, Advances in water treatment by adsorption technology, *Nat. Protoc.*, 1 (2006) 2661–2667.
 [2] M.T.M. Pendergast, E.M.V. Hoek, A review of water treatment membrane nanotechnologies, *Energy Environ. Sci.*, 4 (2011) 1946–1971.

[3] Z. Yuan, S. Xie, X. Yu, Y. Pan, S. Li, J. Liu, P. Du, Physical-chemical property and filtration mechanism of the porous polyvinyl chloride composite membrane as filter for waste water treatment, *Desal. Wat. Treat.*, 105 (2018) 35–40.
 [4] A. Perez-Vidal, J. Diaz-Gomez, J. Castellanos-Rozo, O.L. Usaquen-Perilla, Long-term evaluation of the performance of four point-of-use water filters, *Water Res.*, 98 (2016) 176–182.
 [5] M.N. Chong, B. Jin, C.W.K. Chow, C. Saint, Recent developments in photocatalytic water treatment technology: a review, *Water Res.*, 44 (2010) 2997–3027.
 [6] L.L. Fang, B. Valverde-Perez, A. Damgaard, B.G. Plosz, M. Rygaard, Life cycle assessment as development and decision support tool for wastewater resource recovery technology, *Water Res.*, 88 (2016) 538–549.
 [7] Z.J. Ren, A.K. Umble, Water treatment: Recover wastewater resources locally, *Nature*, 529 (2016) 25–25.
 [8] D. Bastani, N. Esmaili, M. Asadollahi, Polymeric mixed matrix membranes containing zeolites as a filler for gas separation applications: a review, *J. Ind. Eng. Chem.*, 19 (2013) 375–393.
 [9] M. Rawat, V.K. Bulasara, Synthesis and characterization of low-cost ceramic membranes from fly ash and kaolin for humic acid separation, *Korean J. Chem. Eng.*, 35 (2018) 725–733.
 [10] P. Saini, V.K. Bulasara, A.S. Reddy, Performance of a new ceramic microfiltration membrane based on kaolin in textile industry wastewater treatment, *Chem. Eng. Commun.*, 206 (2019) 227–236.
 [11] G. Singha, V.K. Bulasara, Preparation of low-cost microfiltration membranes from fly ash, *Desal. Wat. Treat.*, 53 (2015) 1204–1212.
 [12] H. Kaura, V.K. Bulasara, R.K. Gupta, Preparation of kaolin-based low-cost porous ceramic supports using different amounts of carbonates, *Desal. Wat. Treat.*, 57 (2016) 15154–15163.
 [13] H. Kaur, V.K. Bulasara, R.K. Gupta, Effect of carbonates composition on the permeation characteristics of low-cost ceramic membrane supports, *J. Ind. Eng. Chem.*, 44 (2016) 185–194.
 [14] W. Li, W. Xing, N. Xu, Modeling of relationship between water permeability and microstructure parameters of ceramic membranes, *Desalination*, 192 (2006) 340–345.
 [15] M.D.M. Innocentini, V.C. Pandolfelli, Permeability of porous ceramics considering the klinkenberg and inertial effects, *J. Am. Ceram. Soc.*, 84 (2001) 941–944.
 [16] P. Zhang, L. Hu, J.N. Meegoda, Pore-scale simulation and sensitivity analysis of apparent gas permeability in shale matrix, *Materials*, 10 (2017) 104–106.
 [17] M.D.M. Innocentini, P. Sepulveda, V.R. Salvini, V.C. Pandolfelli, Permeability and structure of cellular ceramics: a comparison between two preparation techniques, *J. Am. Ceram. Soc.*, 81 (1998) 3349–3352.
 [18] Q. Zhang, W. Jing, Y. Fan, N. Xu, An improved Parks equation for prediction of surface charge properties of composite ceramic membranes, *J. Membr. Sci.*, 318 (2008) 100–106.
 [19] M.A. Hubbe, N. Wu, O.J. Rojas, S. Park, Permeation of a cationic polyelectrolyte into mesoporous silica. Part 2. Effects of time and pore size on streaming potential, *Colloids Surf., A*, 364 (2010) 7–15.
 [20] J.V. Nicolini, C.P. Borges, H.C. Ferraz, Selective rejection of ions and correlation with surface properties of nanofiltration membranes, *Sep. Purif. Technol.*, 171 (2016) 238–247.
 [21] Z. Ma, M. Wang, X. Gao, C. Gao, Charge and separation characteristics of nanofiltration membrane embracing dissociated functional groups, *Front. Environ. Sci. Eng.*, 8 (2014) 650–658.
 [22] B. Xu, J. Chen, Z. Yuan, L. Zhang, Y. Fang, Simulation analysis on the profiles of droplets wetting on the substrates, *J. Disper. Sci. Technol.*, 36 (2015) 1816–1824.
 [23] B. Yu, J. Li, A geometry model for tortuosity of flow path in porous media, *Chin. Phys. Lett.*, 21 (2004) 1569–1571.
 [24] Q. Zhang, Y. Fan, N. Xu, Effect of the surface properties on filtration performance of Al₂O₃-TiO₂ composite membrane, *Sep. Purif. Technol.*, 66 (2009) 306–312.